ELSEVIER

Analytica Chimica Acta 337 (1997) 5–28

ANALYTICA CHIMICA ACTA

Voltammetric investigation of the complexation equilibria in the presence of a low level of supporting electrolyte Part 1: Steady-state current–potential curves for inert complexes

Marcin J. Pałys[a,b,*], Zbigniew Stojek[a], Martinus Bos[b], Willem E. van der Linden[b]

[a] *Laboratory of Theory and Application of Electrodes, Department of Chemistry, University of Warsaw, Pasteura 1, 02-093 Warsaw, Poland*
[b] *Laboratory for Chemical Analysis, Department of Chemical Technology, Twente University of Technology, P.O. Box 217, 7500 AE Enschede, Netherlands*

Received 8 1996; revised 23 1996; accepted 7 1996

Abstract

The use of microelectrodes for voltammetric investigations of the complexation equilibria at very low concentrations of supporting electrolyte allows the risk of competitive complexation or contamination to be avoided, makes the activities of the species involved closer to their concentrations (which facilitates comparisons with the spectroscopic results) and finally, allows the concentrations of the species to be varied over a broader range. This paper presents the calculations of the steady-state currents for a wide range of complexes that are inert on the experimental time scale, and reports the influence of the concentration of the electroinactive ionic species on the limiting currents. Also, for a number of cases the variation of halfwave potential with the ligand concentration, resulting from changes in the ohmic drop, is given. It is assumed that only one species (the complex or the uncomplexed form) is electroactive; if this is the complex, it may or may not change the number of ligands. The theoretical results were obtained either employing the Myland–Oldham theory extended in this paper or by digital simulation. The results of calculations show that the magnitude of the changes in the steady-state limiting current on complexation depends on the type of complexation equilibrium, the type of the change in the reactant charge number in the electrode process, and the complex formation constant. In a number of situations migrational effects are negligibly small and no special treatment is necessary, despite the lack of supporting electrolyte. In other cases, where migration is significant, the relations between the measured steady-state limiting current and the complex formation constant β are given in the form of fitted equations that can be used to obtain β from appropriate experimental data.

Keywords: Inert complexes; Voltammetry; Migration; Low ionic strength

1. Introduction

Application of microelectrodes in the absence or in the presence of a very small amount of supporting electrolyte opens up new possibilities for voltammetric and amperometric investigations in new areas (monitoring of concentrations of various species during liquid–liquid extraction [1], detection in supercritical fluid chromatography [2]) or under unusual conditions (e.g., stripping analysis for traces of metals in very pure water [3,4]). It has been

* Phone: +48 22 22 0211 ext. 269, Fax: +48 22 22 5996, e-mail: mpalys@chem.uw.edu.pl.

PII S0003-2670(96)00288-7

recently shown that such measurements have interesting analytical aspects [5–8]. Since the position and the height of the voltammetric waves depend, in different ways for different parameters of the electrode reaction, on the concentration of supporting electrolyte; these changes can be employed for mechanistic [9,10] and thermodynamic studies. For this purpose a rigorous theory is needed.

There is a substantial progress in the theoretical description of voltammetric waves obtained in the absence of deliberately added supporting electrolyte [11–18], however, the discussed cases are limited to simple electrode reactions ($R \rightarrow P$) and equal diffusion coefficients of the product and the reactant. More complicated situations are treated in papers recently published on electrode reactions of weak acids [19,20]. In this paper, we deal with a novel application of voltammetry in the absence of deliberately added supporting electrolyte: the study of complexation equilibria. We intend to present a theoretical model useful for such studies.

The investigation of complexation reactions by electrochemical methods has a long history. Despite the well-known methodology used, a number of unsolved problems still remain. Many of these problems come from the need to work in solutions containing a sufficient excess (at least 50 times) of supporting electrolyte. The ions of the electrolyte can be involved in side reactions (even if the stability constants of the side reaction products are low, the relatively high concentration of these ions can change the equilibrium concentrations to a significant extent) or sufficiently high concentrations of supporting electrolyte may not be attained. An addition of supporting electrolyte also changes the ionic strength of the solution and the activities of the investigated species. Because of these problems, the stability constants determined electrochemically are often not comparable to those measured using spectroscopic methods where no electrolyte is added.

The elimination of supporting electrolyte excludes a risk of competitive complexation reactions, relaxes the problems of supporting electrolyte solubility, makes the activities of the involved species closer to their concentrations, and probably brings spectroscopically- and voltammetrically-determined equilibrium constants closer to each other. The price for this modification is a complication of the transport model to the electrode—both diffusion and migration now have to be considered. However, this approach offers an additional advantage: the diffusion–migration model of the transport allows the value of the *IR*-drop to be calculated explicitly. The usual instrumental corrections of experimental results for the ohmic drop (based on approximate and not always reliable models) are then no longer necessary.

The fact that no supporting electrolyte is added to the investigated system does not imply that the sample contains no electrolyte at all. If the ligand is an ion, excesses of the free ligand, uncomplexed form and ligand's counterion act as supporting electrolyte, increasing the solution conductivity and decreasing the extent of migration of the species present in the solution.

We focus our attention on both inorganic inert systems (like transition metal hydroxo complexes, and inert complexes of platinum(IV), chromium and cobalt in non-aqueous media [21]), as well as on organic host–guest systems, where steric hindrances prevent the metal-containing guest ion or molecule from leaving the host cavity, thus inhibiting the dissociation (e.g., hemicarcerands, hemispherands, spherands, calixspherands etc.).

In this paper, we demonstrate how the absence of deliberately added supporting electrolyte influences the steady-state *I–E* curves and what effects can be observed with respect to the height, position and symmetry of the wave. The presented equations are the best fits to the theoretically calculated data that relate the stability constant to the limiting current and to the concentration of the ligand. These relations should help in understanding the phenomena observed experimentally and allow a system of diagnostics to be developed to determine the stoichiometry of a complex and the complex formation constant.

2. Theory

2.1. Basic assumptions

We consider a system in which complexation of species A takes place according to the reaction

$$A^{z_A} + nL^{z_L} \Leftrightarrow AL_n^{z_A+nz_L}$$

characterized by the complex formation constant

$$\beta_n = \frac{[AL_n^{z_A+nz_L}]}{([A^{z_A}][L^{z_L}]^n)}$$

The dissociation reaction is supposed to be so slow that during the voltammetric experiment the equilibrium is frozen and no significant change in the concentrations of the species takes place as a result of a homogeneous reaction in the solution. In addition to A, L and AL_n, the solution contains only counterions (if possible, only one type of counterion), and no supporting electrolyte is added. Only one of the species, A or AL_n is electroactive. If the electrode reaction proceeds without the decomposition of the product, it is assumed that the redox couple formed is reversible and that both forms are soluble. The products of the electrode reaction are not involved in any homogeneous equilibria that could change their concentrations to a significant extent on the time scale of the experiment.

The geometry of the working electrode is hemispherical and the concentric counterelectrode is large and remote. We assume that the double layer thickness can be neglected with respect to the diffusion layer thickness. This is the case when the size of the electrode is not much less that 1 μm and the total ion concentration is not much less than 10^{-6} M [17] (wh.ch is the usual lowest level in 'pure' solvents). This allows us to assume that local electroneutrality is satisfied at all points in the solution.

Transport to a hemispherical electrode is a one-dimensional problem and therefore, this geometry has been chosen. Simulations for the much more popular disk electrodes would require calculations for two-dimensional systems. For transport involving migration, this is associated with significant mathematical complications, and will be the subject of the future paper. Nevertheless, the steady-state currents for a disk electrode usually can be approximated with reasonable accuracy by hemispherical electrode currents multiplied by $2/\pi$.

Finally, we will assume that the Nernst–Einstein equation relating the mobility of an ion to its diffusion coefficient is obeyed and that the diffusion coefficient of each species is constant and does not vary with the distance from the electrode.

2.2. Calculation of stability constants of inert complexes

The classical approach to the electrochemical determination of stability constants of inert complexes is based on the analysis of the currents (limiting currents or peak currents) recorded for a series of equilibrated solutions containing species A and L in various ratios, in the presence of the excess of supporting electrolyte. The variation of the current forms the basis for the computation of the stability constant. For the case of steady-state voltammetry at microelectrodes and a complexation reaction, as considered in this paper, the stability constant can be determined from the equations that are derived by combining the mass balances with the definition of the stability constant:

$$1 - \tilde{c}_A^{eq} - \tilde{\beta}_n \tilde{c}_A^{eq} (\tilde{c}_L^{tot} - n(1 - \tilde{c}_A^{eq}))^n = 0 \quad (1)$$

if only form A is electroactive, or

$$\tilde{c}_{AL_n}^{eq} - \tilde{\beta}_n (1 - \tilde{c}_{AL_n}^{eq})(\tilde{c}_L^{tot} - n\tilde{c}_{AL_n}^{eq})^n = 0 \quad (2)$$

if only form AL_n is electroactive. Concentrations $\tilde{c}_i^{eq}$ are bulk equilibrium concentrations normalized with respect to the total concentration of form A, $\tilde{c}_i^{eq} = c_i^{eq}/c_A^{tot}$, $\tilde{c}_L^{tot}$ is the total (analytical) concentration of species L normalized with respect to c_A^{tot}, and the normalized n-th stability constant $\tilde{\beta}_n$ is defined as $\tilde{\beta}_n = (c_A)^n \beta_n$. Each equation has no general analytical solution but it can be solved using an iterative procedure like, for example, the Newton method. The equilibrium concentration of A or AL_n, appearing in these equations needs to be determined from the value of the current. If the electrolyte is in excess, the necessary proportionality constants can be computed from the limiting currents: the constant for A from the current measured when the concentration of L equals zero, and the constants for AL_n from the current measured for a sufficiently high concentration of L.

If the supporting electrolyte is not present in sufficient excess, the relationship between the steady-state limiting current and the electroactive species concentration is not straightforward. To relate the experimentally obtained currents to concentrations of the electroactive species and in consequence, to

determine the $\beta_n$value, one should use the theory accounting for migrational effects.

As a consequence of the normalization method, the normalized stability constant $\tilde{\beta}_n$ depends on the concentration of the species A raised to the power n. This means that the results obtained for $\tilde{\beta}_n = 1000$ correspond to a system where $\beta_n = 1000$ and $c_A = 1\,M$ as well as to one where $\beta_n = 10^6$ and $c_A = 10^{-3}\,M$.

2.3. Existing methods for computation of I–E curves under diffusion–migration conditions

Because it is assumed that the complex formed is inert, we can consider the system as consisting of a single electroactive component and a number of electroinactive ionic species acting as the supporting electrolyte. The theory developed by Myland and Oldham [16] allows steady-state *I–E* curves to be computed if one assumes that (i) the electrode reaction involves a single reactant and a single, soluble product, (ii) the diffusion coefficients of the reactant and the product are equal, and (iii) the supporting electrolyte ions are singly charged. The requirement of the solubility of the product can be omitted [4]. However, important limitations of the original theory and all its modifications are the requirements of 'single reactant–single product' reaction and the assumption of equal diffusion coefficients of reactant and product. Particularly, for electrode reactions leading to a decomposition of the complex reactant (with full or partial liberation of the ligand), more than one product is formed, and there can be a large difference in the diffusion coefficients between the reactant and some of the products. It is possible to extend the theory of Myland and Oldham to cover the cases of complicated supporting electrolyte compositions, where various electroinactive ions are present, and there are no restrictions on their charges or diffusion coefficients. Such an extension is useful from the application point of view to systems with complex formation equilibria and it is described in following sections.

The alternative approach to solve the diffusion–migration problem is digital simulation of the transport. A number of papers appeared on this topic: Norton et al. [17] modelled the transport to the electrode inside the double layer, accounting for the migration in the unscreened electric field originating from the electrode. Smith and White [18] simulated steady-state *I–E* curves for the 'one reactant–one product' case (D_R=D_P) under conditions where the double layer is much thicker than the diffusion layer. Another paper of Norton et al. [22] mentions a method of simulation applicable to complicated reaction schemes, with no restrictions on the diffusion coefficients, but the authors do not give any detail of the method or present any results for these more complicated cases.

In our previous paper [23], we have described a simulation scheme that can be used for the modelling of the steady-state *I–E* curves for any type of the electrode reaction that is not coupled to a homogeneous equilibrium (at least on the time scale of the electrochemical experiment), with no restrictions imposed on the charges and the diffusion coefficients of ions. That method was based on the simulation of the time-dependent concentration profiles under chronopotentiometric conditions at a hemispherical electrode.

From the discussed methods, digital simulation [23] is the most universal because it imposes the least number of restrictions on the reaction scheme, ion charges and diffusion coefficients, but it is also relatively time-consuming. On the contrary, extended Myland–Oldham method can be applied only to some classes of reactions involving complex compounds, but it requires the minimum number of calculations. Therefore, in this paper the extended method is used whenever possible, while digital simulation is used in all other cases. Details of these two approaches are discussed below.

2.4. Extension of the Myland–Oldham solution

After assuming that the solution contains a single reactant, possibly a single product of the electrode reaction, and a number of electroinactive ions (denoted with subscript i) having charges z_i and diffusion coefficients D_i, it is possible to follow the philosophy of the Myland–Oldham derivation and to relate the mole fraction (or the concentration) of each ion to the normalized electric potential, $\Psi = F\Phi/RT$. The transport equations for the reactant (index R), the product (index P), and for the ions of supporting

electrolyte (subscript i), under the steady-state conditions, can be written as

$$dx_R + z_R x_R d\Psi = \frac{-I}{2\pi nFD_R} d(1/r) \approx \frac{-I}{2\pi nFD} d(1/r) \quad (3)$$

$$dx_P + z_P x_P d\Psi = \frac{I}{2\pi nFD_P} d(1/r) \approx \frac{I}{2\pi nFD} d(1/r) \quad (4)$$

$$dx_i + z_i x_i d\Psi = 0 \quad (5)$$

where x_k is the mole fraction of species k, r is the distance from the electrode center, and other symbols have their usual electrochemical meaning. The last equation shows that the steady-state profiles of electroinactive ions are independent of their diffusion coefficients D_i; summation of Eqs. (3)–(5) confirms that the principle of total uniform concentration, $x_R + x_P + \sum x_i = 1$ holds.

Integration of Eq. (5) gives

$$x_i = x_i^{bulk} \exp(-z_i \Psi) \quad (6)$$

Using the electroneutrality condition $z_R x_R + z_P x_P + \sum z_i x_i = 0$ and the principle of the total uniform concentration ($c_R + c_P + \sum_i c_i = c^{total,bulk}$ at each point in the solution), the mole fractions of the reactant and the product can be expressed in terms of fractions of the supporting electrolyte ions:

$$x_R = \frac{z_P}{z_P - z_R}\left(1 - \sum_i x_i\right) + \frac{1}{z_P - z_R}\sum_i z_i x_i \quad (7)$$

$$x_P = \frac{-z_R}{z_P - z_R}\left(1 - \sum_i x_i\right) - \frac{1}{z_P - z_R}\sum_i z_i x_i \quad (8)$$

The summation of weighted equations, $(z_P - z_R)$•[Eq. (4)]+$(z_i - z_R)$•[Eq. (5)], leads to cancellation of all dx_i terms; the subsequent substitution of x_P by the right-hand side of Eq. (8) leads to the expression

$$\left[\sum_i (z_P z_R + z_i(z_i - z_P - z_R) x_i^{bulk} \exp(-z_i \Psi)) - z_P z_R\right] d\Psi = (I/2\pi FDc_{total}^{bulk}) d(1/r) \quad (9)$$

which links the current to both the electric potential and the concentration of inert ions. By integration of this expression one can calculate the value of Ψ as a function of current intensity I:

$$z_P z_R \Psi + \sum_i \left(\frac{z_P z_R}{z_i} + z_i - z_P - z_R\right) x_i^{bulk}[\exp(-z_i \Psi) - 1] = -I/2\pi rFDc_{total}^{bulk} \quad (10)$$

The expression for the limiting value of Ψ, Ψ^L, can be obtained from Eq. (7) by setting x_R to zero and substitution of x_i with the right-hand side of Eq. (6):

$$\sum_i (z_p - z_i) x_i^{bulk} \exp(-z_i \Psi^L) - z_P = 0 \quad (11)$$

Unlike the simple case considered by Myland and Oldham, Eqs. (10) and (11) have no general analytical solution and should be solved numerically. To calculate the value of the limiting current, Ψ^L should be obtained from Eq. (11) and inserted into Eq. (10), which in turn delivers the current density value. To compute a complete I–E curve for the systems with well-defined electron transfer type the value of Ψ should be varied between 0 and Ψ^L, and the corresponding currents and concentrations of the reactant and the product should be computed. The value of the electrode potential that corresponds to the chosen Ψ can be calculated using Eqs. (40)–(44) from the original paper of Myland and Oldham [16].

Eqs. (6)–(8), (10) and (11) use molar fractions of ions, similarly to [16]. They can be easily converted to a more usual form in which the concentrations normalized with respect to the bulk concentration of the reactant, $\tilde{c}_k = c_k / c_R^{bulk}$, are used:

$$\tilde{c}_R = \frac{z_P}{z_P - z_R}\left(\sum_j \tilde{c}_j^{bulk} - \sum_i \tilde{c}_i\right) + \frac{1}{z_P - z_R}\sum_i z_i \tilde{c}_i \quad (12)$$

$$\tilde{c}_P = \frac{-z_R}{z_P - z_R}\left(\sum_j \tilde{c}_j^{bulk} - \sum_i \tilde{c}_i\right) - \frac{1}{z_P - z_R}\sum_i z_i \tilde{c}_i \quad (13)$$

$$\tilde{c}_i = \tilde{c}_i^{bulk} \exp(-z_i \Psi) \quad (14)$$

$$z_P z_R \Psi \sum_j \tilde{c}_j^{bulk} + \sum_i \left(\frac{z_P z_R}{z_i} + z_i - z_P - z_R\right) \tilde{c}_i^{bulk} \times [\exp(-z_i \Psi) - 1] = -I/2\pi rFD\tilde{c}_R^{bulk} \quad (15)$$

$$\sum_i (z_P - z_i) c^{bulk}{}_i \exp(-z_i \Psi^L) - z_P \sum_j \tilde{c}_j^{bulk} = 0 \quad (16)$$

where the sums over i cover all supporting electrolyte ions (i.e., ions not involved in the electrode process), and the sums over j cover all species that are transported (i.e., the reactant, the product, and all other ionic species present in the solution).

If the product is uncharged and the solution contains only the reactant and a counterion, the equation for the limiting current simplifies to the form

$$\sum_i (z_i - z_R)\tilde{c}_i^{bulk} = I/2\pi rFD\tilde{c}_R^{bulk} \quad (17)$$

The so-called support ratio, $SR=c_{supp.electr}/c_R$ is extensively used by Myland and Oldham because the migrational effects can often be presented as a single-value function of this parameter. This convenient relation is only valid, however, for the systems with 1 : 1 electrolyte and single charged counterions, all with the same diffusion coefficients. Therefore, the support ratio cannot be used, e.g. to compare migrational effects in a redox systems in two supporting electrolytes with different ionic charges. For such situations, the use of the ionic strength ratio, $\sum_{i\neq R} z_i^2 c_i / z_R^2 c_R$, is a better choice, although it cannot be used for systems with $z_R=0$ and still no single-value relation exists between this parameter and the magnitude of the migration effects.

2.5. Simulation method

The method of simulation, described in [23], is based on the modelling of chronopotentiometric experiments at hemispherical electrodes. If the time of the experiment becomes very large, the system approaches a steady-state. From a series of such chronopotentiograms, computed for various current densities, steady-state I–E curves can be obtained.

The scheme can be applied to any electrode reaction of the type

$$n_1R_1 + n_2R_2 + \ldots \xrightarrow{ne^-} m_1P_1 + m_2P_2 + \ldots$$

where the number of the reactants and the products and their stoichiometric coefficients can adopt any value. There is no restriction on the diffusion coefficients and on the charges of species present in the solution, whether electroactive or not.

The simulation method has been tested and proved to have a good performance and accuracy when the support ratio was higher than 0.01. Because in the studies of complexation processes the situation where the support ratio is lower than this value should be seldom encountered, this simulation scheme can be employed in all cases where the extended Myland–Oldham method cannot be used.

3. The calculation procedure and the software

The input data set was made of bulk (analytical) concentrations, charges, diffusion coefficients, the equation for the homogeneous reaction(s), and the stability constant(s). Unless otherwise stated, all diffusion coefficients were set equal to the diffusion coefficient of the reactant.

The calculation procedure essentially consisted of two basic steps: in the first one, equilibrium concentrations of all species in the considered mixtures of A and L were calculated using the initial bulk concentrations and the value of $\tilde{\beta}_n$. In the second step, the steady-state I–E curve was computed using either the extended Myland–Oldham method or digital simulation. From this curve, the limiting current I_{lim} and halfwave potential $E_{1/2}$ were determined. The latter parameter was calculated under assumption that the electron transfer step is reversible, and only for systems for which such an assumption was reasonable.

These two steps were then repeated for various ratios of ligand/A concentrations and for various $\tilde{\beta}_n$, and results were used to construct plots of I_{lim} vs. c_L and $\tilde{\beta}_n$, as well as plots of $E_{1/2}$ vs. c_L and $\tilde{\beta}_n$ (where applicable).

To calculate the actual concentrations of species under conditions of homogeneous equilibrium, the software described in detail in [24], rewritten in C, was used.

The program for the calculation of steady-state I–E curves was written in the C programming language (ANSI C) which ensures its portability to virtually every computer platform. The program is capable both of computing the results using the extended Myland–Oldham scheme and of simulating I–E curves. The simulation routine, employing the Crank–Nicolson method, was essentially the same

as previously described [23]. To reduce the computation time, an exponentially expanding space grid was used with the increments increasing according to the modified Feldberg's function $\rho = \ln(1 + 3(\tilde{R} - 1))$ [25]. The time increment was increased according to the exponential function $\delta\tilde{T} = \exp(\delta\tau/2)$, unless the system was likely to begin to oscillate. These two transformations drastically reduced the number of grid points and time steps necessary to approach the steady-state. Typically, the number of space grid points employed was a few hundred, and the number of time increments used to simulate the steady-state could be as low as a few tens.

All simulations were carried out using CRAY Y-EL 98 computer. Calculations of the extended Myland–Oldham solutions were done on an IBM PC-compatible computer (80486 processor).

4. Results and discussion

For an investigation of homogeneous equilibria, the important questions are: (i) what is the effect of the addition of the ligand on the limiting current value and on the halfwave potential, and how large are the deviations from symmetry of the wave, and (ii) how to compute the stability constant from the steady-state diffusion–migration currents?

The answers to these questions depend on the category of the reaction. The complex formation reactions where both A and L species are uncharged are not considered here because such systems do not exhibit any migrational effects, so these reactions, even in the absence of the supporting electrolyte can be treated using the classical methods for the determination of stability constants and complex stoichiometry, based on the limiting current measurement.

To limit the number of combinations of the charge numbers of ions and the types of the electrode processes that should be considered, one can take advantage of the symmetry of the migrational effects and of the equivalence of some particular cases.

The symmetry rule can be applied when the charge numbers of ions are taken with the opposite sign and the type of the electrode reaction is reversed, e.g. from reduction to oxidation. If this is so, the corresponding plots remain the same and only the potential shift and current change their signs.

Electron transfer processes can be considered equivalent if they differ from each other only in the number of uncharged products. For example, the two reactions below

$$R^{z_R} \rightarrow P^{z_P} + (z_P - z_R)e$$

$$R^{z_R} \rightarrow P^{z_P} + N1 + N2 + (z_P - z_R)e$$

where $N1$ and $N2$ are uncharged products, cannot be distinguished by analysis of I–E curves. Important consequences of the equivalence of electrode reactions are visible in the case of charge reversal processes, where the reactant and the product are ions with opposite signs. Such processes are extremely rare and if present, they are usually coupled to a parallel comproportionation reaction that strongly influences the transport of the reactant. However, among the electrode reactions of complexes, there are processes which do not follow the true single-step charge reversal scheme, but do have identical characteristics. Consider the system

$$A^{2-} + HL^{+} \Leftrightarrow AHL$$

$$AHL^{-} \rightarrow AL + H^{+} + 2e$$

where anion A^{2-} is complexed by the protonated form of the ligand, HL^{+}. After the single-step transfer of two electrons the neutral product AL is formed and the H^{+} ion is released. Because AL does not influence the transport of other species, the reaction has the characteristics of a charge reversal process. Systems like the one described above can be found among organic molecules exhibiting binding properties toward anions.

In the following sections, as a rule, the charge of species A is assumed to be positive. Although some combinations of ion charges can then seem improbable as far as complexation of simple ions are concerned, examples of such reactions (or their symmetric versions) can sometimes be found among complexation processes involving macrocycles and metallomacrocycles on one hand, and small cations (organic or inorganic), anions or small molecules on the other hand.

4.1. Types of electrode processes involving complex compounds

Generally, there are three situations that can be encountered during the studies of electrode reactions of complexes: (i) the complex is reduced (or oxidized) without change in the number of ligands (outer sphere electron transfer); (ii) the electrode reaction proceeds with a total or a partial decomposition of the complex and the liberation of the ligands; and (iii) the uncomplexed form is electroactive, while the complex is not.

In the case of complexes that do not change the number of ligands after electron transfer, the original or the extended Myland–Oldham theory can be used because these systems satisfy the theoretical assumptions. In such situations, the diffusion coefficients of the reactant and the product usually don't differ significantly, although systems that involve a uncharged reactant or product can deviate from this rule.

When the uncomplexed form is electroactive, the complexation process changes the support ratio and in this way it influences the steady-state *I–E* curves. In this case, however, there is a greater possibility that the diffusion coefficients D_R and D_P may differ because molecules of uncomplexed species are often smaller than those that are complexed. Also, the changes in solvation of differently charged ions can lead to larger variations of diffusivities.

The most complicated reactions are those in which the number of ligands changes. The extended Myland–Oldham theory does not apply here and the simulation approach has to be used.

4.2. Electroactive complex: reactions without change of the number of ligands

4.2.1. Variation of the support ratio

The support ratio (SR) is a useful parameter for predicting the magnitude of migrational effects. Analysis of its variation allows the domains of stability constant $\tilde{\beta}_n$ and c_L/c_A concentration ratios in which the migrational effects can be significant to be found. If the complex formed is the only electroactive species in the considered potential range, the supporting electrolyte consists of the free ligand, the uncomplexed form (if each one is charged), and the counterions. Fig. 1 shows how the support ratio depends on the concentration of the ligand. Three situations are considered: both the ligand and uncomplexed form are charged (Fig. 1A),

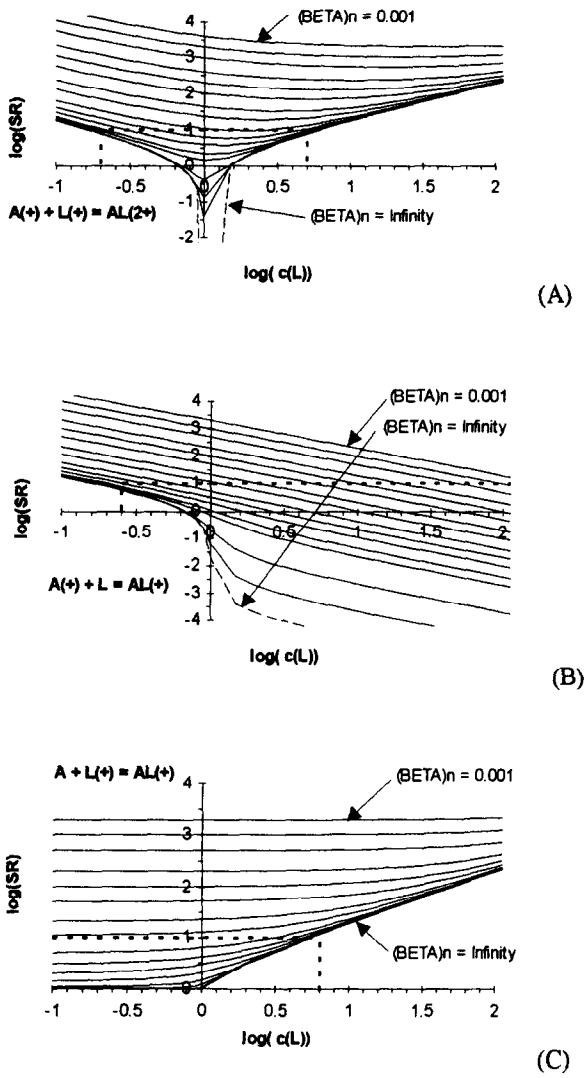

Fig. 1. Dependence of the support ratio on the ligand concentration and the stability constant of the complex; the complex is the electroactive species. (A) all forms charged ($A^+ + L^+ = AL^{2+}$), (B) neutral ligand ($A^+ + L^0 = AL^+$), (C) only ligand charged ($A^0 + L^+ = AL^+$). Lines are drawn for values of normalized formation constant ($\tilde{\beta}_n$) equal to 0.001, 0.002, 0.004, 0.01, 0.02, 0.04, 0.1, 0.2, 0.5, 1, 2, 5, 10, 100, 1000, 10 000 and ∞. Migration effects are most likely to be seen inside the area marked with the dotted line.

the ligand is uncharged (Fig. 1B), or the uncomplexed form is uncharged (Fig. 1C).

It can be seen in the figure that all plots consist of two regions: $c_L \leq n \cdot c_A$ and $c_L > n \cdot c_A$. In the first region the SR vs. c_L line decreases if the species A is charged, and increases if it is not. The first effect is caused by a progress of the conversion of A to AL_n and an associated decrease of the c_A/c_{AL} ratio. In the second situation, the support ratio increases due to the presence of the increasing amount of free ligand and the ligand counterion in the solution.

In the region $c_L > n \cdot c_A$, the support ratio either increases (charged ligand) or continues to decrease (uncharged ligand). Variations in the SR in this region are simply determined by the presence of an excess of the ligand which, if charged, works as supporting electrolyte. If the ligand is uncharged, the decrease in SR is due to the further decrease in c_A/c_{AL}.

The magnitude of the migrational effect is closely related to the support ratio. It becomes noticeable when the SR value is roughly less than 10. The dotted lines in Fig. 1 mark the regions where migration is likely to be seen; these regions are $-0.7 < \log c_L < 0.7$, $\log\tilde{\beta}_n > 0$ for both A and L charged; $\log c_L < 0.8, \log\tilde{\beta}_n > -0.3$for uncharged species A, and $\log c_L < 0.8, \log\tilde{\beta}_n > -0.4$for the uncharged ligand case. In the last case (Fig. 1B), the SR can theoretically acquire any value but it is reasonable to limit the considerations to the situation when $c_L/c_A \leq 100$.

4.2.2. Limiting current

The overall change of the limiting current with an increase in the c_L/c_A ratio is superposition of two effects: the increase of the complex concentration and the enhancement (or the diminution) of the transport due to the migrational effect. The way the limiting current varies as a result of the migrational effect depends on the variation of the support ratio (differently for charged and uncharged ligand), charge of the reactant (the complex), and charge of the product. A migrational decrease of the limiting current is observed when the electrode reaction leads to a product with higher charge number. A migrational increase takes place when the electrode reaction is accompanied by a charge decrease, charge cancellation or a sign reversal. When the complex is not charged, the height of the steady-state wave is not influenced by migration. The value of the steady-state currents for the considered cases can be computed using the extended Myland–Oldham theory.

As was already mentioned, the fact whether A or L is charged (or both) determines the c_L range in which the migrational effects can be observed. When both species (A and L) are charged, the migrational enhancements and diminutions are observed for large $\tilde{\beta}_n$ values and a ligand concentration close to $n \cdot c_A$. The enhancements will be reflected as peaks (Fig. 2A), while diminutions (Fig. 2B) appear as biased 'plateaus' ($c_L > n \cdot c_A$) on line $I_{lim} - \log(c_L)$ plots. An explanation for the appearance of the peak-shaped curves is as follows: if almost all A is converted to the complex and the support ratio is low, the migrational effects raises the wave plateau above that expected for purely diffusional transport. A further addition of the ligand has little effect on the concentration of the complex but it increases the support ratio and decreases the effect of the migration. The computation results show that the migrational effect on the limiting steady-state current is fairly small for the charge increase of decrease reactions. It is moderate for charge cancellation processes, and most pronounced in the case of charge reversal, where the current enhancements due to the migration are the greatest.

If the ligand is uncharged, migration becomes significant when almost all A is converted to AL_n, i.e. when $c_L \geq n \cdot c_A$. Then the I_{lim}–$\log(c_L)$ plots have a sigmoidal shape with the value of the normalized steady-state limiting current asymptotically approaching the value predicted by the theories of Amatore et al. and Myland and Oldham for the complete absence of the supporting electrolyte. The predicted values are less than 1 for charge increase reaction (Fig. 2C) and greater than 1 for charge decrease or charge cancellation reactions (Fig. 2D). Since the current for the sign-reversal reaction, theoretically, it has an infinitely large value for SR=0, a sigmoidal plot with a sloped plateau is obtained for this case (Fig. 2E) and the currents are much greater than in Fig. 2D. It should be noted that traces of impurities that increase the SR value will have an insignificant effect on the currents shown in Fig. 2C and D, but the plot in Fig. 2E will eventually level off when the concentration of impurities starts to determine the value of the support ratio.

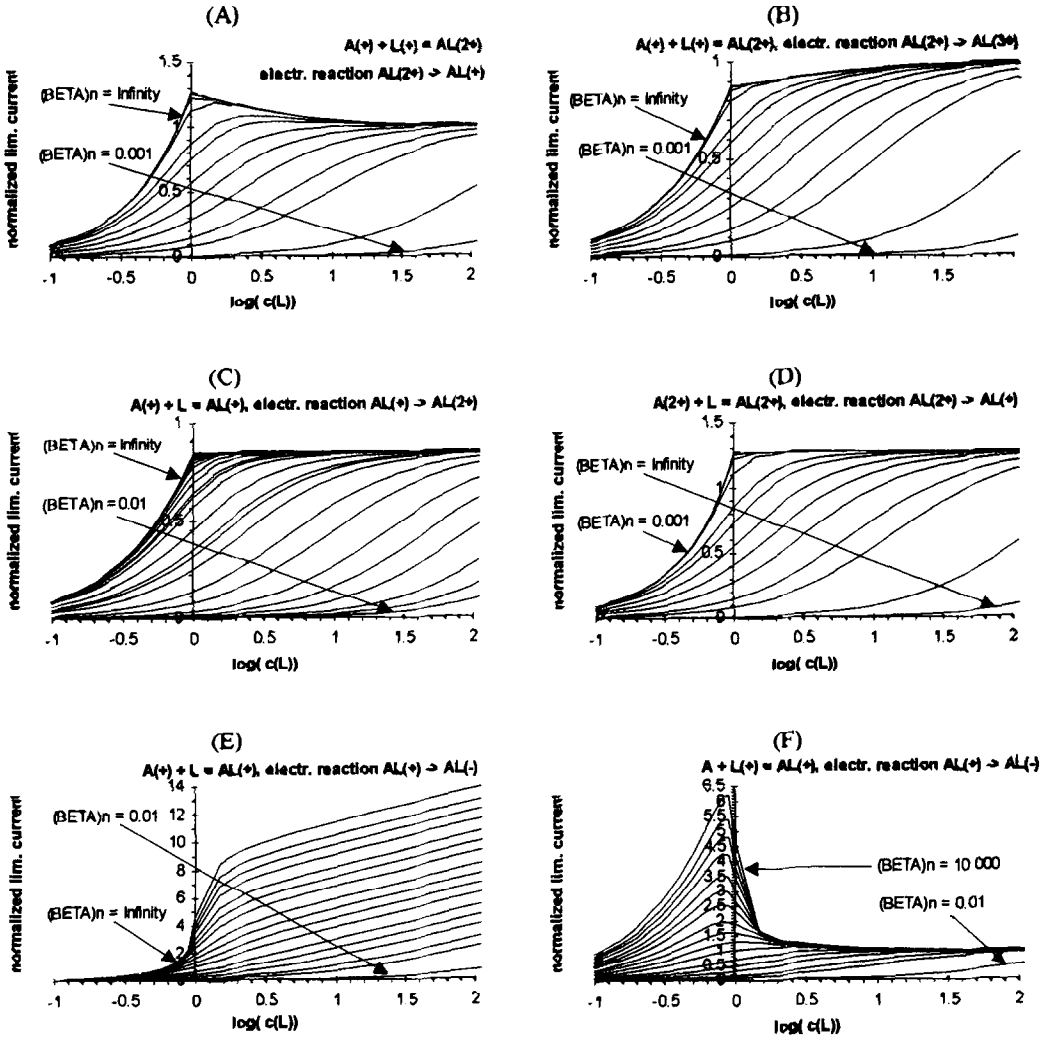

Fig. 2. Dependence of the normalized limiting current on the normalized ligand concentration and the stability constant $\tilde{\beta}_n$ of the complex for a number of instances of homogeneous equilibria and electrode reactions. Lines in figures A, B, C, D are drawn for $\tilde{\beta}_n$ equal to 0.001, 0.01, 0.1, 0.2, 0.5, 1, 2, 5, 10, 100, 1000, 10 000 and ∞, and in figures E and F for $\tilde{\beta}_n$ equal to 0.01, 0.1, 0.2, 0.5, 1, 2, 5, 10, 20, 40, 100, 200, 400, 1000, 2000, 4000 and 10 000.

In the last case, if A is neutral and L is charged, the migrational effects are most pronounced for $c_L < n \cdot c_A$. When the reaction type is the charge enhancement, a sloped sigmoidal plot (similar to one in Fig. 2B) is obtained. The charge decrease and charge cancellation reactions lead to peak-shaped curves, similar to ones in Fig. 2A. If the reaction is a sign-reversal process, the characteristic asymmetric peak is observed for high $\tilde{\beta}_n$ values (Fig. 2F): just before the ligand concentration reaches $n \cdot c_A$, the normalized steady-state limiting current sharply drops to the value close to 1.

If the complex is not charged, migration does not influence the transport of the reactant and the obtained I_{lim} vs. c_L curves represent the sole effect of the change in the complex concentration.

4.2.3. Halfwave potential and wave symmetry

If it is assumed that the electrode process is reversible and both redox forms are soluble, it is

possible to examine the variations of the halfwave potential. Generally, for unimolecular reactions the variation of $E_{1/2}$ is independent of the complex concentration and it is entirely determined by the support ratio (Fig. 3).

If both A and L are charged, the plot has a peak-like shape with the extremity corresponding to the minimum value of the support ratio (Fig. 3A, B). The shift of the halfwave potential is of the order of a few mV, with exception for the charge cancellation reaction and the sign-reversal scheme, whereas shifts are up to ca. 30 mV and above 100 mV, respectively.

If L is uncharged and A charged, the halfwave potential is shifted from $E^{0\prime}$ for $c_L < n \cdot c_A$, and then approaches the reversible halfwave potential for an excess of the ligand (Fig. 3C and D). Maximum shifts do not exceed a few mV, except for the charge cancellation and sign-reversal reactions.

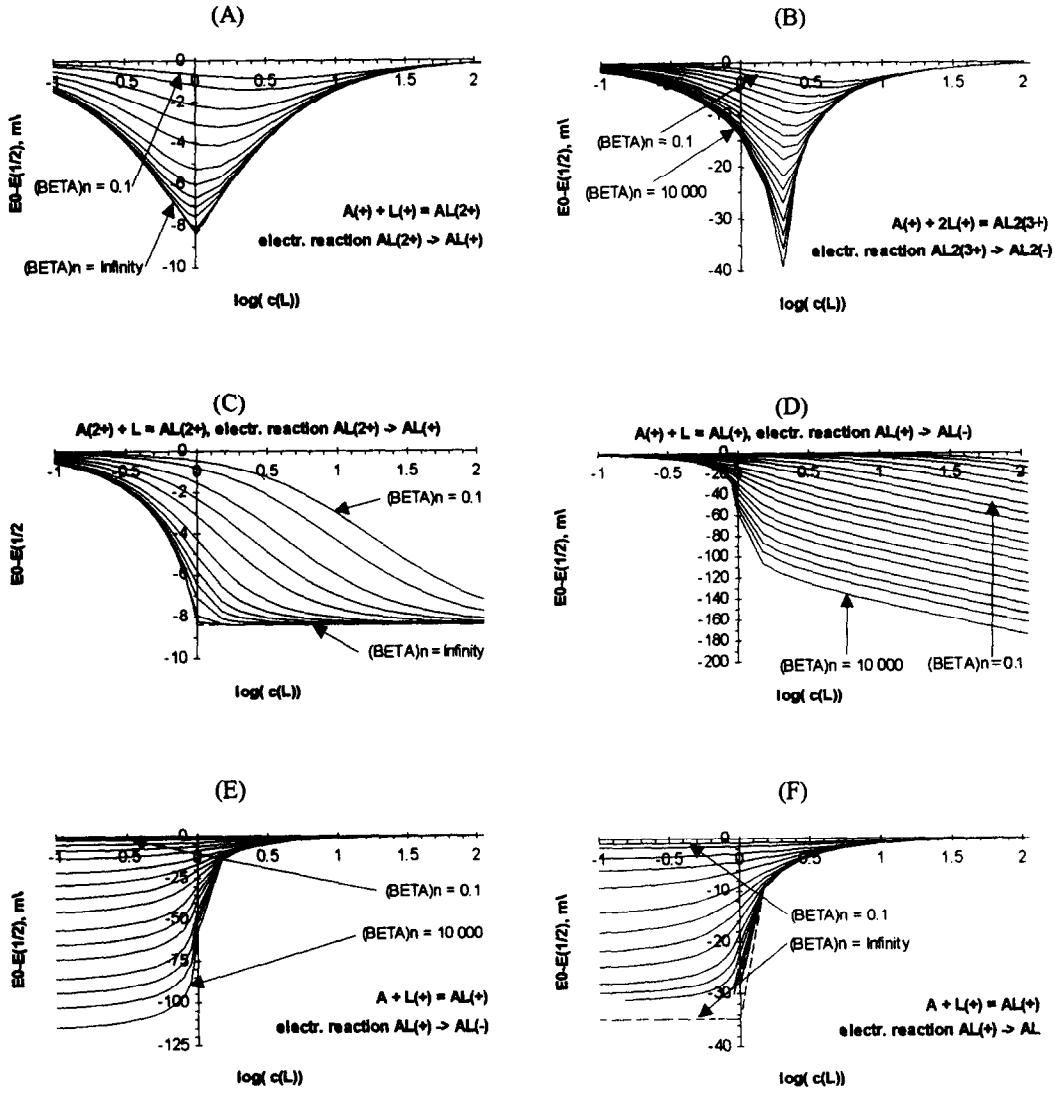

Fig. 3. Dependence of halfwave potential on the ligand concentration and the stability constant of the complex for a number of instances of homogeneous equilibria and electrode reactions. Lines in figures are drawn for $\tilde{\beta}_n$ values 0.1, 0.2, 0.5, 1, 2, 5, 10, 20, 40, 100, 1000 and 10 000, in figures C, D, E and F additionally for $\tilde{\beta}_n$ 200, 400, 2000 and 4000.

In the opposite case (*A* uncharged, Fig. 3E and F), the curves are almost like the mirror images of the previous plots. If the concentration of the ligand is lower than $n \cdot c_A$ the halfwave potential is shifted from $E^{0\prime}$ value, the shift is small (few mV) except for the charge cancellation and sign-reversal reactions. The characteristic feature of the latter case is that there is no theoretical limit on the potential shift and it can increase infinitely with $\tilde{\beta}_n$ value (i.e., the support ratio may be infinitely low). When the ligand concentration becomes larger than $n \cdot c_A, E_{1/2} - E^{0\prime}$ rapidly decreases and becomes zero.

The above discussion is only valid when both redox forms are soluble. If the product of the electrode reaction is deposited on the surface, it is likely that $E^{0\prime}$ will change due to the blocking of the electrode, or a change in the reaction mechanism."

The migrational effects almost always result in a deformation of the voltammetric steady-state wave. Because migration is more intensive at higher current densities, its impact on the foot of the wave is smaller than on the wave top. If the migration impedes the transport, the upper half of he wave is more extended along the *E* axis and its slope decreases; if the migration enhances the transport, the upper part of the curve is shrunk and has a higher slope than the lower part. Additional deformation comes from the *IR*-drop effect. The asymmetry of the wave can be measured as a difference between the potential of the inflection point (E_{infl}) of the *I–E* curve and the halfwave potential. It appears from the calculation that the effect of asymmetry measured in this manner would be of the order of a fraction of a mV and therefore, it wouldn't be noticed experimentally. The only exception is the case of charge cancellation and sign-reversal reactions, where (most probably) due to the larger *IR*-drop, E_{infl} differs from $E_{1/2}$ by a few mV (<10).

4.3. *Electroactive complex: reactions with liberation of the ligand*

In this category, the chemical equilibrium is identical to that previously discussed and all considerations regarding the support ratio (and the plots from Fig. 1) apply to this case too. The difference lies in the fact that electrode reaction is not unimolecular and therefore, the principle of the total uniform concentration (and consequently both the original and the extended Myland–Oldham theory) do not apply. The results for the steady state currents can be obtained by digital simulation of the transport to the electrode [23].

Another difference is that it is rather improbable that a reaction leading to the decomposition of an inert complex would be reversible in the electrochemical sense. Assumption of irreversibility, however requires that at least two additional parameters (α and k_s) have to be considered, which makes the full analysis unfeasible. Therefore, we will consider limiting steady-state currents only and we will deal neither with the halfwave potentials nor the wave symmetry.

In spite of these differences it happens that results obtained for electrode reactions with the liberation of the ligand (e.g., $AL_3^{3+} \rightarrow AL_2^{2+} + L^+$) and without liberation (e.g., $AL_3^{3+} \rightarrow AL_3^{2+}$) do not differ from each other. Therefore, in the following discussion the processes with product decomposition will be always compared to corresponding cases from the previous category, i.e. reactions without change in the number of ligands (outer-sphere electron transfers).

The fact that the product is decomposed does not influence the diffusional component in the transport of the reactant to the electrode but it can influence the migrational component if the component if the conductivity of the solution is changed. Because solution conductivity is equal to $(F^2/RT)\sum_i z_i^2 c_i D_i$, in order to find out whether the liberation of the ligand influences the steady-state limiting current one should compare the concentration, charge and diffusivities of the product(s) in the cases of reactions with and without ligand liberation.

At this point it is clear that when the ligand uncharged, its liberation does not change the number of charge carries in the solution and therefore, no change in the conductivity is observed. Systems like the two below:

SystemI	System II
Homogeneous equilibrium:	Homogeneous equilibrium:
$A^{z_R} + nL \Leftrightarrow AL_n^{z_R}$	$A^{z_R} + nL \Leftrightarrow AL_n^{z_R}$
Electrode reaction:	Electrode reaction:
$AL_n^{z_R} \rightarrow AL_n^{z_P} + (z_P - z_R)e^-$	$AL_n^{z_R} \rightarrow AL_n^{z_P} + (n-m)L + (z_P - z_R)e^-$

will behave identically. This is an illustration of the equivalent processes mentioned earlier in this paper.

If one assume that the diffusion coefficients of charged species are all equal (what has been done in calculations in this paper) the conductivity of the solution will be influenced by the ligand liberation only when

$$\left(\sum_{\text{all P}} z_P^2 c_P\right)_{\text{no liberation}} \neq \left(\sum_{\text{all P}} z_P^2 c_P\right)_{\text{liberation}}$$

An example of a set of systems where no difference in the transport of the reactant is expected is given in Table 1 (reactions A1 and A2), because in both cases $\sum z_P^2 c_P$ for the right-hand side of the electrode reaction equals to c. This is not the case when reactions B1, B2 and B3 are considered (Table 1), where $\sum z_P^2 c_P$ for the reaction B3 is three times greater than that for reaction B2. It is necessary to emphasize that the consideration based on the $\sum z_P^2 c_P$ are approximate and valid only under assumption of equal diffusion coefficient of the charged product species.

If $\sum z_P^2 c_P$ is larger, the migrational effects will be diminished; if the sum is smaller, the influence of the migration on the study-state current will be stronger. Certainly, in system where migration does not influence the transport rate (uncharged reactant), the steady-state currents will be the same for both reactions (although the influences on the halfwave potentials may differ).

Table 1
Examples of homogeneous equilibria and electrode reactions with and without the liberation of the ligand

Homogeneous equilibrium	Electrode reaction	Reaction symbol
$A^- + 2L^+ \Leftrightarrow AL_2^{3+}$	$AL_2^{3+} + 2e^- \rightarrow AL_2^+$	A1
	$AL_2^{3+} + 2e^- \rightarrow AL + L^+$	A2
	$AL_2^{3+} + 2e^- \rightarrow A^- + 2L^+$	A3
$A + 2L^+ \Leftrightarrow AL_2^{2+}$	$AL_2^{2+} + e^- \rightarrow AL_2^+$	B1
	$AL_2^{2+} + e^- \rightarrow AL + L^+$	B2
	$AL_2^{2+} + e^- \rightarrow A^- + 2L^+$	B3
$A + 2L^+ \Leftrightarrow AL_2^{2+}$	$AL_2^{2+} + 3e^- \rightarrow AL_2^-$	C1
	$AL_2^{2+} + 3e^- \rightarrow AL^{2-} + L^+$	C2
	$AL_2^{2+} + 3e^- \rightarrow A^{3-} + 2L^+$	C3

Fig. 4 presents the calculation results for the reactions from Table 1. Each plot shows the difference between the steady-state limiting current for the reaction with partial (or total) liberation of the ligand, and the steady-state limiting current for outer-sphere electron transfer, both normalized with respect to the latter. It can be seen that differences shown in Fig. 4A1 and B1 are essentially zero; the noise comes from imprecision in the simulation. This is the result that can be expected on the basis of conductivity change considerations: the $\sum z_P^2 c_P$ for the pairs of reactions A1–A2 and B1–B2 (Table 1) are the same. This is not the situation when more ligand molecules are liberated (pairs A1–A3 and B1–B3, Table 1): the conductivity increases and the migrational enhancement of the current gets smaller. Generally, the differences shown are within a few percent of the outer-sphere I_{lim}.

Another situation can be observed in Fig. 4C. Each reaction from this set (Table 1 C1, C2 and C3) changes the conductivity in a different way, therefore, the corresponding currents are always different. Because the outer-sphere reaction is a charge reversal process, the measured currents are significantly influenced by the variation in the conductivity, which is visible in the figure.

4.4. Electroactive uncomplexed form

This is the last category of reactions considered here. The complex formed is an electroinactive species and the effect of the complexation influences the I–E curves in two ways: directly, by lowering the concentration of the electroactive species, and indirectly, by changing the support ratio and thus migrational contributions. Because electrode reactions belonging to this category are essentially one reactant–one product processes, the electric variable can be calculated using the extended Myland–Oldham theory.

4.4.1. Variation of the support ratio

With an increase in the ligand concentration ratio of the uncomplexed to complexed forms monotonically decreases. Because either the complex, or the ligand (or both) are charged, the support ratio always increases and for a large excesses of the ligand the contributions from the migration effects become

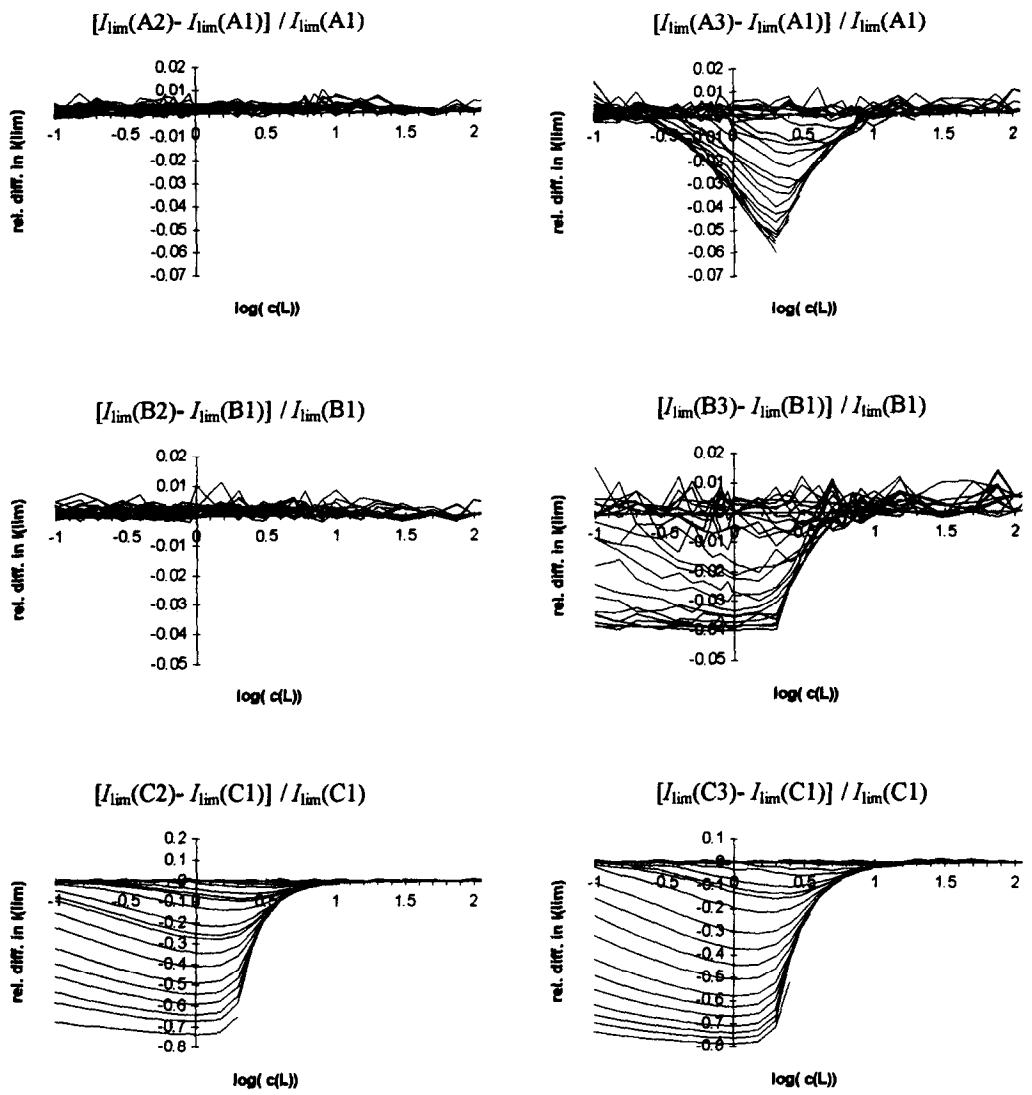

Fig. 4. Relative difference of limiting steady-state currents of reaction with and without liberation of the ligand, normalized with respect to the latter. Symbols of reaction equations refer to Table 1. $\tilde{\beta}_n$ values vary from 0.001 up to 10 000.

negligible and the system behaves as a well-supported one (the case of uncharged A and L is excluded).

The variation of the support ratio in Fig. 5. The rate of the transition from the diffusion–migration of the sole diffusion transport depends on the charges of the species involved in the complexation reaction. If both A and L are charged (Fig. 5A, B), the transition is relatively fast. It is slower when the ligand is uncharged (particularly if the stability constant is small Fig. 5C). If A is uncharged (Fig. 5D), the support ratio for $c_L < n \cdot c_A$ can be very small.

4.4.2. Limiting current

In general, one can expect that the limiting current will decrease upon addition of the ligand, as the primary effect is a decrease in the concentration of the electroactive species. This decrease will be faster if the migration slows down the transport to the electrode (reactions leading to ions with the higher

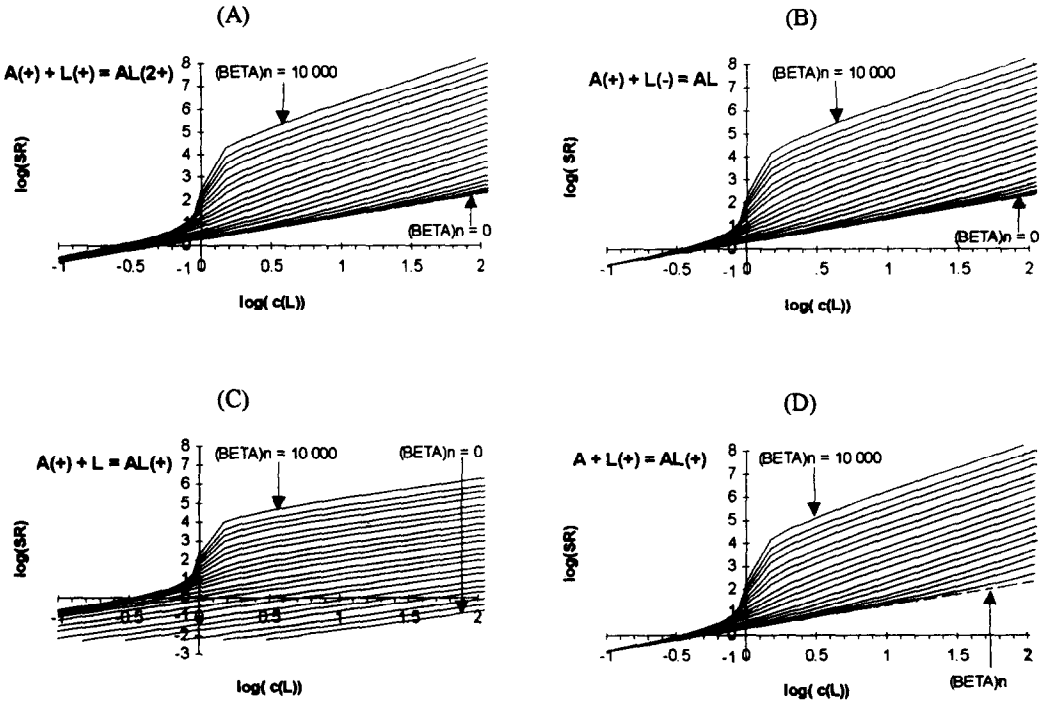

Fig. 5. Dependence of the support ratio on the ligand concentration and the stability constant of the complex; the uncomplexed form is the electroactive species. (A) reaction $A^+ + L^+ = AL^{2+}$, (B) reaction $A^+ + L^- = AL^0$, (C) reaction $A^+ + L^0 = AL^+$, (D) reaction $A^0 + L^+ = AL^+$. Lines are drawn for values of normalized formation constant $\tilde{\beta}_n$ equal to 0, 2, 5, 10, 30, 100, 300, 1000 and 10 000.

charge numbers) and slower if the transport is enhanced by the migration (the charge decrease, charge cancellation and sign reversal reactions).

The migrational effects are always best visible in low ligand concentration ranges, where the support is small (Fig. 6). These effects can either increase the current (Fig. 6A, C, D) or decrease it (Fig. 6B). If the ligand is a uncharged molecule and the stability constant is small, the influence of migration can be observed even for large excess of the ligand (Fig. 6C and D).

Some of I_{lim}–$\log(c_L)$ lines pass through a maximum (Fig. 6B). They are observed when the stability constant $\tilde{\beta}_n$ is small, the ligand is charged and the migration impedes the transport. An addition of the ligand to a solution of pure A significantly increases the support ratio, but it hardly influence the concentration of free A. As a result, the current increases due to elimination of migration. A further addition of the ligand eventually decreases the concentration of A and the observed current.

4.4.3. Halfwave potential and wave symmetry

If reversible charge transfer is assumed, one can examine the variation of the halfwave potential of the steady-state I–E curve versus amount of the added ligand. The shift of $E_{1/2}$ with respect to $E^{0\prime}$ of the reacting system is small (1–2 mV) for charge increase processes and moderate (<10 mV) for charge decrease reactions. For the charge production, charge cancellation and sign reversal processes, the shift is of order of tens of mV (Fig. 7). These changes are caused by the variation of the IR-drop and by the changes, influenced by migration, in the ratio of the reactant and the product concentrations at the surface of the electrode.

If the product of the reversible electrode reaction forms an amalgam, the reaction should follow the trend observed for charge cancellation processes, as the amalgamated product is not charged and does not alter the transport of other species. It can be expected, however, that side effects like the saturation of the electrode during the steady-state experiment may

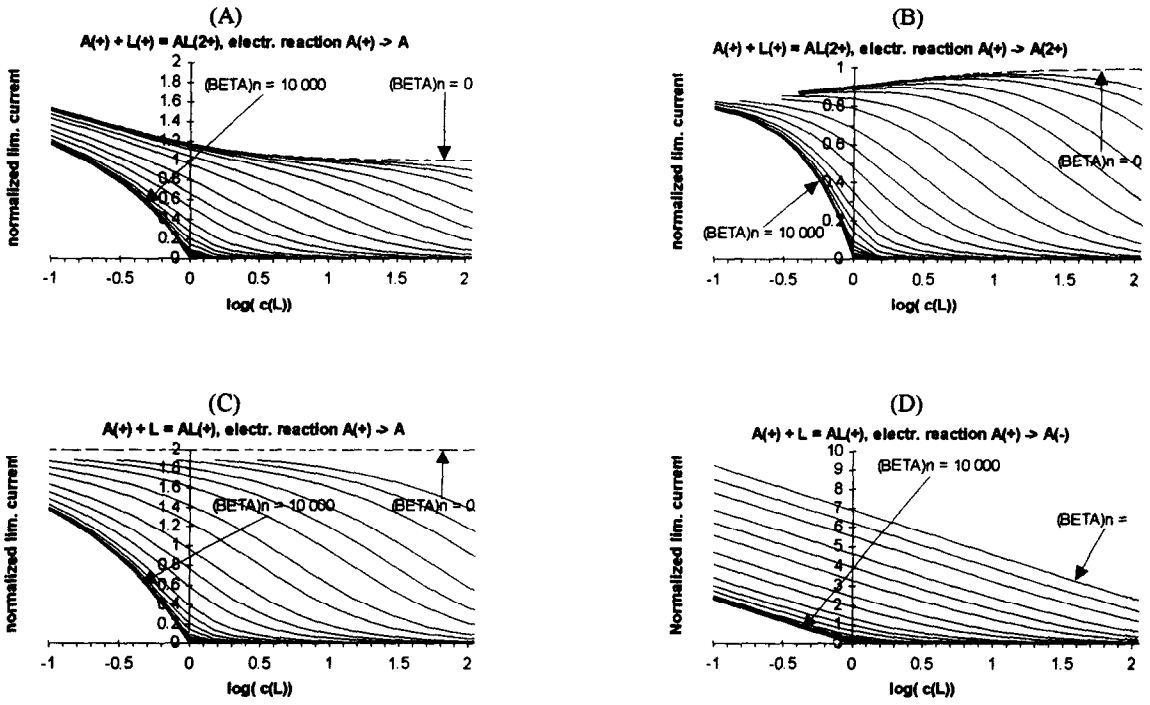

Fig. 6. Dependence of the normalized limiting current on the ligand concentration and the stability constant of the complex: (A) equilibrium $A^+ + L^+ = AL^{2+}$, electrode reaction $A^+ \rightarrow A'^0$; (B) equilibrium $A^+ + L^+ = AL^{2+}$, electrode reaction $A^+ \rightarrow A^{2+}$; (C) equilibrium $A^+ + L = AL^+$, electrode reaction $A^+ \rightarrow A'^0$; (D) equilibrium $A^+ + L = AL^+$, electrode reaction $A^+ \rightarrow A^-$. Lines are drawn for values of normalized formation constant $\tilde{\beta}_n$ equal to 0 (dashed line), 1, 2, 5, 10, 30, 100, 1000 and 10 000.

alter the mechanism of the process and influence the halfwave potential. This is also valid for processes where the product of the reaction is deposited on the solid electrode forming a layer on its surface. In these cases, it is unlikely that the presented theory correctly predicts the way the halfwave potential varies.

The wave symmetry is hardly influenced by migrational effects when the reaction type is charge decrease or charge increase. In the range of ligand concentrations studied, the asymmetry parameter $E_{infl} - E_{1/2}$ is smaller than 3 mV and therefore, the experimentally recorded curves can be considered as symmetric. The asymmetry is slightly larger for the sign reversal reaction and more significant (ca. 12 mV) for the charge cancellation reaction.

On the basis of the Myland–Oldham model, it can be expected that the observed steady-state currents will be independent of the diffusion coefficients of the supporting electrolyte ions. In the considered category of reactions the complex is electroniactive and it belongs to the supporting electrolyte species. A difference in the diffusion coefficients between the free and the complexed forms should have no influence on the steady-state I–E curves.

4.5. *Effect of migration on the calculation of β*

Because the influence of migration is not always easy to detect on the steady-state I–E and I_{lim}–$\log(c_L)$ curves, the migrational effect can be overlooked and an apparent stability constant calculated. It should be emphasized that such simplifications can cause significant errors in the calculations of β, particularly for very small and very large constants.

If the complex is the only electroactive species, the enhancement of its transport intensity results in higher currents and leads to overestimation of the stability constant. When the rate of the transport is lower, due to migration, the values of β obtained from

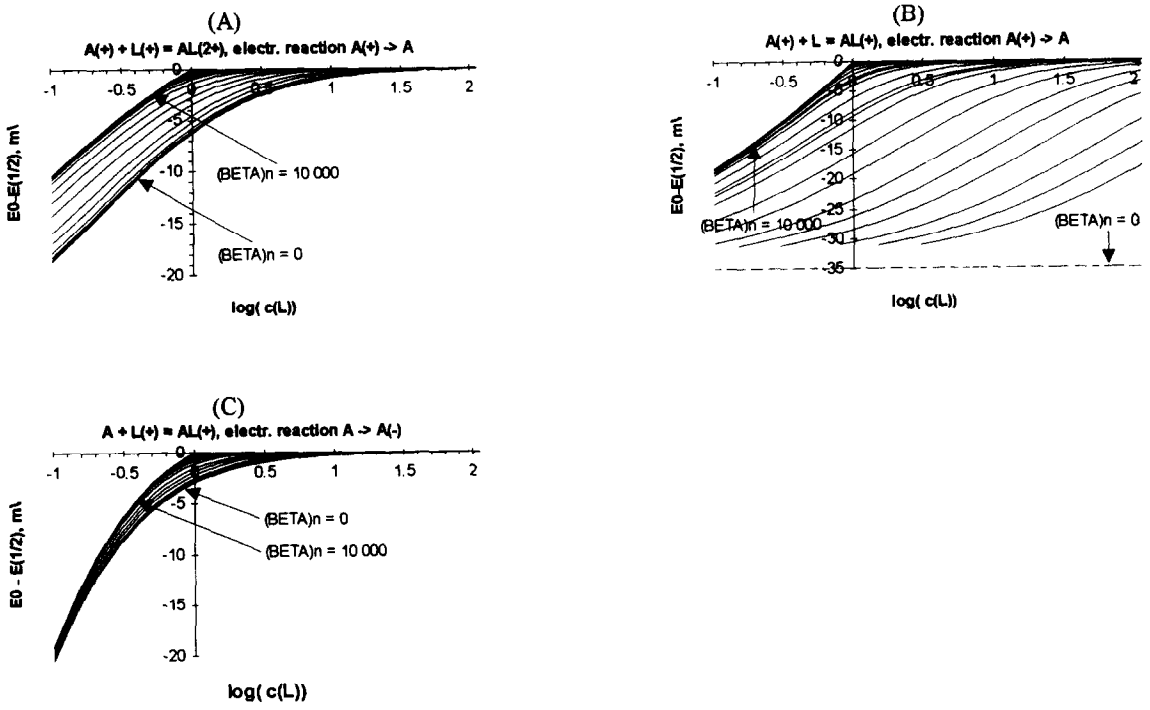

Fig. 7. Dependence of the normalized halfwave potential on the ligand concentration and the stability constant of the complex: (A) equilibrium $A^+ + L^+ = AL^{2+}$, electrode reaction $A^+ \rightarrow A'^0$; (B) equilibrium $A^+ + L = AL^+$, electrode reaction $A^+ \rightarrow A'^0$; (C) equilibrium $A^0 + L^+ = AL^+$, electrode reaction $A^0 \rightarrow A'^-$. Lines are drawn for values of normalized formation constant $\tilde{\beta}_n$ equal to 0 (dashed line), 1, 2, 5, 10, 30, 100, 1000 and 10 000.

the uncorrected limiting current data are underestimated. In certain situations it is clear that the migration cannot be neglected and the usual method of calculations of β will not work. Such a situation happens, for example, when a maximum is present on the I_{lim}–$\log(c_L)$ curve. If currents are not corrected for migration effects, a negative value of β is obtained for the curve for which I_{min} exceeds unity.

If the uncomplexed form is electroactive, the decrease of the current caused by the migration results in higher apparent stability constants. If the current is enhanced, the apparent β is lower than the real one. Unfortunately, in comparison to the reactions of electroactive complexes, the evidence of migrational contributions to the transport are less visible here.

4.6. *Fitted equations for the calculation of stability constants*

To facilitate calculations of the stability constants on the basis of the migrational–diffusional limiting currents, an approximate function has been found to relate $\tilde{\beta}_n$ to $\tilde{I}_{lim}$ for a certain ligand concentration. Such a function depends on the combinations of ion charges and on the type of the electrode reaction, but is the same for symmetric and equivalent mechanisms, as described earlier. The form of this function is

$$\log\tilde{\beta}_n = p_0 + p_1\log\tilde{I}_{lim} + p_2\log(\tilde{I}_{\beta=\infty} - \tilde{I}_{lim}) \qquad (18)$$

for the case of the electroactive complex. If the uncomplexed form is relectroactive, the form of the function is

$$\log\tilde{\beta}_n = p_0 + p_1\log(\tilde{I}_{lim} - \tilde{I}_{\beta=0}) + p_2\log(\tilde{I}_{\beta=\infty} - \tilde{I}_{lim}) \qquad (19)$$

where p_0, p_1, p_2, $\tilde{I}_{\beta=0}$ and $\tilde{I}_{\beta=\infty}$ are the reaction-dependent parameters, and $\tilde{I}_{lim}$ is the normalized limiting steady-state curve observed at the considered concentration of the ligand.

For each type of reaction, the parameters are computed for relative concentrations of the ligand

Table 2
Parameters for fitted approximation function for $\tilde{\beta}_n$ for the selection of instances of reactions of the complex

Equilibrium	Electrode reaction	c_L/c_A	p_0	p_1	p_2	$\tilde{I}_{\beta=\infty}$
$A^+ + L^+ \Leftrightarrow AL^{2+}$	$AL^{2+} + e^- \rightarrow AL^+$	0.5	0.1912	1.0556	−1.0837	0.5885
		1	0.2421	1.0111	−2.0531	1.27495
	$AL^{2+} + e^- \rightarrow A + L^+$	20	−1.2813	1.0059	−1.007	1.024
		100	−1.991	1.0076	−0.9981	1.00496
	$AL^{2+} \rightarrow AL^{3+} + e^-$	0.5	0.0758	1.0593	−1.0896	0.4522
		1	−0.1141	0.9987	−1.9953	0.8799
		20	−1.2906	1.0144	−1.0004	0.9787
		100	−1.9931	1.0106	−0.9977	0.9952
	$AL^{2+} + 2e^- \rightarrow AL$	0.5	0.3319	1.0625	−1.091	0.7682
		1	1.9979	1.0103	−4.1068	3
		20	−1.2736	1.0032	−1.0096	1.05
		100	−1.9969	0.9973	−1.0031	1.01
	$AL^{2+} \rightarrow A^{2+} + L^+ + e^-$	0.5	0.7373	1.1206	−0.8105	0.4475
		1	0.1964	1.0857	−1.5868	0.865
		20	−2.777	1.0787	−0.8967	0.98
		100	−4.6529	0.9811	−1.0564	1
	$AL^{2+} + 2e^- \rightarrow A^- + L^+$	0.5	0.7040	1.0645	−1.0361	0.71
		1	1.2213	1.0257	−2.0669	1.695
		20	−2.9033	1.0146	−0.9945	1.05
		100	−4.8338	0.883	−1.1804	1.02
$A^+ + 2L^+ \Leftrightarrow AL_2^{3+}$	$AL_2^{3+} + e^- \rightarrow AL_2^{2+}$	0.5	−0.5219	1.0176	−2.1031	0.2763
		1	−0.4467	1.0383	−2.2213	0.5725
		20	−2.4956	1.1361	−0.9962	1.0338
		100	−3.9885	0.8893	−1.004	1.0074
	$AL_2^{3+} \rightarrow AL_2^{4+} + e^-$	0.5	−0.6812	1.0122	−2.0837	0.2329
		1	−0.6726	1.0317	−2.2069	0.4581
		20	−2.5236	1.1289	−1.0009	0.9712
		100	−3.9767	1.1829	−0.9969	0.9929
	$AL_2^{3+} + 3e^- \rightarrow AL_2$	0.5	−0.2332	1.0344	−2.2264	0.3804
		1	0.1906	1.07499	−2.5231	1.0126
		20	−2.6714	0.6347	−1.1069	1.1156
		100	−3.9547	1.3579	−0.9905	1.0226
	$AL_2^{3+} + 4e^- \rightarrow AL_2^-$	0.5	−0.0482	1.0431	−2.3029	0.4612
		1	0.71299	1.0945	−2.7513	1.5094
		20	−2.6498	0.6329	−1.1097	1.1608
		100	−3.9682	1.0149	−0.9982	1.0304
	$AL_2^{3+} + 2e^- \rightarrow AL_2^+$	0.5	−0.3961	1.0247	−2.1443	0.3171
		1	−0.2174	1.0522	2.2833	0.7087
		20	−2.4998	1.0921	−1.0066	1.0726
		100	−3.9769	1.0346	−1.0004	1.0149
	$AL_2^{3+} + 3e^- \rightarrow AL^- + L^+$	0.5	−0.4148	1.0464	−2.0834	0.365
		1	0.2047	1.0909	−2.1626	0.88
		20	−5.6512	1.1517	−0.9655	1.115
		100	−9.5509	-2.4257	−1.0864	1.025

Table 2
(Continued)

Equilibrium	Electrode reaction	c_L/c_A	p_0	p_1	p_2	$\tilde{I}_{d=\infty}$
	$AL_2^{3+} + e^- \rightarrow AL^+ + L^+$	0.5	−1.531	1.0029	−2.3175	0.2825
		1	−1.2836	1.0087	−2.4279	0.5775
		20	−4.8447	1.9057	−0.6444	1.035
		100	−9.7329	−2.3763	−1.1244	1.01
	$AL_2^{3+} \rightarrow AL^{3+} + L^+ + e^-$	0.5	−1.7249	1.0008	−2.1459	0.2337
		1	−2.1095	0.9685	−2.5259	0.4625
		20	−5.9253	1.032	−1.0282	0.97
		100	9.3096	0.0402	−1.0224	0.995
	$AL_2^{3+} + 2e^- \rightarrow AL + L^+$	0.5	−0.8321	1.0308	−2.1095	0.3175
		1	−0.3557	1.0743	−2.1695	0.7075
		20	−5.6778	1.1678	−0.991	1.075
		100	−9.4384	-0.7051	−1.0591	1.015
	$AL_2^{3+} + e^- \rightarrow A + 2L^+$	0.5	−1.5364	1.0019	−2.3202	0.2825
		1	−1.3159	1.0057	−2.4578	0.5775
		20	−6.0839	0.85929	−1.1645	1.04
		100	−9.7329	−2.3763	- 1.1244	1.01
	$AL_2^{3+} \rightarrow A^{2+} + L^+ + e^-$	0.5	−0.5224	1.0957	−1.713	0.23
		1	−1.3841	1.0548	−2.1128	0.4525
		20	−9.2339	−1.6936	−2.1937	0.975
		100	−9.3096	0.0402	−1.0224	0.995
	$AL_2^{3+} + 2e^- \rightarrow A^- + 2L^+$	0.5	−0.6351	1.0475	−1.9934	0.3112
		1	−0.1419	1.1203	−1.975	0.68
		20	−6.6885	0.3062	−1.5013	1.085
		100	−11.5029	−6.7655	−1.7687	1.025
$A^+ + L \Leftrightarrow AL^+$	$AL^+ + e^- \rightarrow AL$	0.5	0.1985	1.0599	−1.0895	0.5859
		1	1.0483	0.9938	−3.5897	2
	$AL^+ + e^- \rightarrow A + L$	20	−0.8618	0.8657	−2.0104	2
		100	−1.6787	0.3285	−2.8321	2
	$AL^+ \rightarrow AL^{2+} + e^-$	0.5	0.0719	1.0569	−1.088	0.454
		1	−0.1548	0.9939	−1.9806	0.849
	$AL^+ \rightarrow A^{2+} + L + e^-$	20	−0.4176	1.6445	0.0779	0.8493
		100	0.9802	4.5447	−0.1543	0.849
	$AL^+ + 2e^- \rightarrow AL^-$	0.5	0.2835	1.0623	−1.0899	0.6932
		1	2.3245	1.2009	−2.8801	4.61022
	$AL^+ + 2e^- \rightarrow A^- + L$	20	2.596	1.3946	−3.2257	12.1549
		100	2.1795	1.7412	−3.3255	13.8056
$A^{2+} + L \Leftrightarrow AL^{2+}$	$AL^{2+} + 2e^- \rightarrow AL$	0.5	0.2268	1.0609	−1.0898	0.619
		1	2.5609	0.9782	−5.4674	3
	$AL^{2+} + 2e^- \rightarrow A + L$	20	−0.1035	0.8604	−2.8667	3
		100	−0.8042	0.6411	−3.0722	3
	$AL^{2+} + e^- \rightarrow AL^+$	0.5	0.1647	1.0577	−1.0869	0.5507
		1	0.2627	1.0156	−2.143	1.274

(Continued)

Table 2
(Continued)

Equilibrium	Electrode reaction	c_L/c_A	p_0	p_1	p_2	$\tilde{I}_{\beta=\infty}$
	$AL^{2+} + e^- \rightarrow A^+ + L$	20	−1.1519	1.0327	−1.0043	1.274
		100	−1.8597	1.0398	−0.9998	1.274
	$AL^{2+} \rightarrow AL^{3+} + e^-$	0.5	0.0816	1.056	−1.087	0.4655
		1	−0.1632	1.0014	−1.3552	0.8799
	$AL^{2+} \rightarrow A^{3+} + L + e^-$	20	−1.1787	1.1346	−0.9035	0.8799
		100	−2.0604	0.7088	−1.0312	0.8799
	$AL^{2+} + 3e^- \rightarrow AL^-$	0.5	0.2836	1.0623	−1.0897	0.6932
		1	2.3245	1.2009	−2.88	4.6102
	$AL^{2+} + 3e^- \rightarrow A^- + L^+$	20	2.5961	1.3946	−3.2259	12.155
		100	2.1803	1.7411	−3.3262	13.8063
$A + L \Leftrightarrow AL^+$	$AL^+ + e^- \rightarrow AL$	0.5	0.3744	1.0286	−1.97996	1
		1	1.0483	0.9938	−3.5897	2
		20	−1.2764	1.0139	−1.0006	1.0128
		100	−1.9857	1.0158	−0.9944	1.0025
	$AL^+ \rightarrow AL^{2+} + e^-$	0.5	−0.0687	1.0269	−1.1858	0.4245
		1	−0.1548	0.9939	−1.9806	0.8491
		20	−1.2903	1.0113	−1.0025	0.988
		100	−2.0032	0.9961	−1.003	0.9975
	$AL^+ + 2e^- \rightarrow AL^-$	0.5	2.3996	1.179	−2.6794	4.2589
		1	2.3245	1.2009	−2.8801	4.6102
		20	−1.2727	1.0124	−1.0014	1.0259
		100	−1.9844	1.0161	−0.9944	1.005
	$AL^+ + e^- \rightarrow A^- + L^+$	0.5	0.5269	1.0543	−1.1223	0.655
		1	0.5353	0.9862	−2.2227	1.31
		20	−2.9867	0.99712	−1.0229	1.015
		100	−4.6547	0.9688	−1.0209	1.005
	AL^+\rightarrow $A^+ + L^+ + e$-	0.5	−0.1532	1.0314	−1.1737	0.415
		1	−0.1333	1.0409	−1.7788	0.83
		20	−3.0315	0.9902	−1.0221	0.99
		100	−4.727	0.9321	−1.0342	1
	$AL^+ + 2e^- \rightarrow A^{2-} + L^+$	0.5	0.6018	1.0322	−1.1431	0.785
		1	1.0472	1.0292	−2.0055	1.57
		20	−2.7803	1.064	−0.8884	1.025
		100	−4.6739	0.9616	−1.0243	1.005

equal to 0.5, 1, 20 and 100, using the calculated model data and the non-linear fitting according to the Marquadt method [26].

Table 2 presents the values for the parameters p_0, p_1, p_2 and $\tilde{I}_{\beta=\infty}$ for a number of reactions where the complex is the electroactive species. The parameter $\tilde{I}_{\beta=\infty}$ is approximately equal to the steady-state limiting current that would be observed if the normalized stability constant $\tilde{\beta}_n$ is infinitely large. This table does not contain entries for the equilibria involving uncharged complexes because their steady-state limiting currents are not influenced by migration and allow the determination of $\tilde{\beta}_n$ by conventional methods.

Table 3 collects the set of parameters for the approximation function for reactions where the

Table 3
Parameters for fitted approximation function for $\tilde{\beta}_n$ for the selection of instances of reactions of the uncomplexed form

Equilibrium	Electrode reaction	c_L/c_A	p_0	p_1	p_2	$\tilde{\beta}_{\beta=0}$	$\tilde{\beta}_{\beta=\infty}$
$A^+ + L^+ \Leftrightarrow AL^{2+}$	$A^+ + e^- \rightarrow A$	0.5	0.0239	−1.0961	1.1604	0.5343	1.2692
		1	−0.06251	−1.9937	0.99998	0.0001	1.1716
		20	−1.28741	−1.0008	1.0276	0	1.0141
		100	−1.99758	−1	1.0092	0	1.0042
	$A^+ \rightarrow A^{2+} + e^-$	0.5	0.1914	−1.0817	1.1025	0.4731	0.8864
		1	0.0235	−2.0193	1.0092	−0.0003	0.9081
		20	−1.2768	−1.0008	1.0268	0	0.9903
		100	−1.9954	−1	1.0091	0	0.9992
	$A^- + 2e^- \rightarrow A$	0.5	−0.0362	−1.1027	1.1802	0.6524	1.6502
		1	0.0002	−1.9927	0.9901	0.0001	1.3862
		20	−1.283	−1.0008	1.0266	0	1.0265
		100	−1.9965	−1	1.0091	0	1.0067
$A^- + 2L^+ \Leftrightarrow AL_2^{3+}$	$A^+ + e^- \rightarrow A$	0.5	−0.6073	−2.0844	1.0499	0.8177	1.2681
		1	−0.6044	−2.2146	1.0720	0.5165	1.1725
		20	−2.5531	−1.0003	1.2653	0	1.0782
		100	−3.9551	−1	0.9666	0	0.9367
	$A^+ \rightarrow A^{2+} + e^-$	0.5	−0.6188.	−2.0753	1.0213	0.6409	0.8861
		1	−0.6125	−2.1797	1.0518	0.4222	0.9083
		20	−2.3849.	−0.9821	0.7175	0	0.710998
		100	−3.6321	−0.9801	0.2705	0	0.0931
	$A^+ + 2e^- \rightarrow A^-$	0.5	−0.6354	−2.1031	1.08298	0.9435	1.6483
		1	−0.5948	−2.2281	1.0786	0.5754	1.3869
		20	−2.55	−1.0003	1.2604	0	1.0901
		100	−3.9811	−0.99999	1.036	0	1.0016
$A^+ + L^- \Leftrightarrow AL$	$A^- + e^- \rightarrow A$	0.5	0.1255	−1.0825	1.1013	0.5857	1.2685
		1	0.0027	−1.9353	0.9872	0.001	1.1715
		20	−1.2873	−1.0008	1.0269	0	1.0141
		100	−1.9976	−1	1.0092	0	1.0042
	$A^+ \rightarrow A^{2+} + e^-$	0.5	0.157	−1.0839	1.10448	0.453925	0.8864
		1	−0.0203	−2.0526	1.00405	−0.00068	0.908
		20	−1.2768	−1.0008	1.02732	0	0.9904
		100	−1.9954	−1	1.00917	0	0.9992
	$A^+ + 2e^- \rightarrow A^-$	0.5	0.0939	−1.0813	1.0983	0.693	1.6487
		1	0.00169	−1.8728	0.9736	0.0019	1.386
		20	−1.2928	−1.0008	1.0268	0	1.0265
		100	−1.9987	−1	1.0092	0	1.0067
$A^{2+} + 2L^- \Leftrightarrow AL_2$	$A^{2+} + 2e^- \rightarrow A$	0.5	0.6348	−0.4832	1.1218	0	1.764
		1	0.2395	−2.9906	0.9944	0	1.536
		20	−0.1598	4.7629	4.2642	0	1.048
		100	0.1253	1.6666	37.0931	0	1.01
	$A^{2+} \rightarrow A^{3+} + e^-$	0.5	4.5979	−0.3533	2.9767	0.6756	0.8367
		1	−0.6115	−2.2055	1.0657	0.4587	0.9046

(Continued)

Table 3
(Continued)

Equilibrium	Electrode reaction	c_L/c_A	p_0	p_1	p_2	$\tilde{\beta}_{\beta=0}$	$\tilde{\beta}_{\beta=\infty}$
		20	−2.4387	−1.0051	0.62454	0	0.71418
		100	−3.9115	−1.0002	0.0702	0	0.0939
	$A^{2+} + 3e^- \rightarrow A^-$	0.5	−0.0471	−2.0665	1.0183	1.8028	2.697
		1	−0.2079	−2.1599	1.0167	0.8031	2.0541
		20	−2.5888	−1.0003	1.2733	0	1.1495
		100	−4.0034	−1	1.0714	0	1.04599
$A^+ + L \Leftrightarrow AL^+$	$A^+ + e^- \rightarrow A$	0.5	−0.268	−1.0606	1.9394	0.5857	2.0033
		1	−0.3437	−1.9023	1.4809	0.0017	1.9684
		20	−1.7254	−0.9996	1.5666	0	1.9313
		100	−2.3763	−0.9999	1.4238	0	1.852
	$A^+ + 2e^- \rightarrow A^-$	0.5	−15.118	−1.0887	11.8765	0.6929	19.9714
		1	−2.6948	−1.8948	2.8526	0	9.5369
		20	−6.1545	−1.0021	4.9789	0	9.5091
		100	−4.0588	−1.001	2.7313	0	5.6779
$A^{2+} + L \Leftrightarrow AL^{2+}$	$A^{2+} + 2e^- \rightarrow A$	0.5	−0.9305	−1.0568	2.7006	0.6188	2.9978
		1	−0.6899	−1.8918	1.758	0.0019	2.8214
		20	−2.1473	−0.9996	1.992	0	2.73298
		100	−2.6972	−0.9999	1.7377	0	2.5351
	$A^{2+} + e^- \rightarrow A^+$	0.5	0.06235	−1.0886	1.1119	0.5505	1.2746
		1	−0.0689	−1.9644	0.98145	0.0006	1.2737
		20	−1.3995	−1.0014	1.0812	0	1.2822
		100	−2.116	−1.0001	1.0806	0	1.2914
	$A^{2+} \rightarrow A^{3+} + e^-$	0.5	0.212	−1.0656	1.1041	0.4654	0.87999
		1	0.0019	−2.0525	0.9978	−0.0008	0.8797
		20	−1.1034	−0.972	0.6848	0	0.6506
		100	−1.8023	−0.9755	0.7412	0	0.6486

electroactive species is the uncomplexed form. The parameter $\tilde{I}_{\beta=0}$ is approximately equal to the limiting steady-state current of A that should be observed if no complex is formed.

In the above formulae, all currents used are normalized using the steady-state diffusion current at the maximum concentration of the electroactive substance as the normalization constant:

$$\tilde{I} = I/I_{\text{norm}} = I/2\pi r_e F D_R c_R^{\text{bulk,max}}$$

where subscript R denotes the uncomplexed from A or the complex AL_n, depending on which is electroactive. Concentration, $c_A^{\text{bulk,max}}$ is simply its total (analytical) concentration, $c_{AL_n}^{\text{bulk,max}}$ is equal to $c_A^{\text{bulk,max}}$ because the highest concentration of AL_n is attained when all A is converted to the complex. To make use of the data from tables, one needs the value of the normalization constants. This value can be obtained in three ways: by direct calculation (provided that r_e, D_R and c_R are available), by measurement under diffusion conditions or by determination from multiple measurements.

The second method can be applied when the complex is electroactive and the ligand is an ion: when an excess of the ligand is added and it can be assumed that practically all A is complexed (i.e., further increase of ligand concentration doesn't increase the current), the measured current is equal to the normalization constant. Migrational effects are absent because the excess of the ligand and its

counterion act as supporting electrolyte present in the sufficient excess. From Fig. 1A and C, it can be seen that for 10-fold excess of the ligand the support ratio is at least 10. Certainly, this method cannot be used when the ligand is uncharged, because then the addition of the ligand decreases the support ratio enhancing the migrational effects (Fig. 1B).

The third method is the most widely applicable. It is based on the measurement of current at two of the ligand concentrations listed in the tables. The system of Eq. (18) or (19), where $\tilde{I}_{\mathrm{lim}}$ is replaced by $I_{\mathrm{lim}}/I_{\mathrm{norm}}$ can be solved by an iterative procedure (e.g. the Newton method) giving the value of $\log\tilde{\beta}_{\mathrm{n}}$.

5. Conclusions

The presented results show that the support ratio in most experiments involving the studies of the complexing equilibria, is not extremely small. Usually, the uncomplexed ligand, free complexed species and all counterions are present at a level sufficient to keep the support ratio above 10. Thanks to that, for the classic method of calculation of the stability constants can be used in many situations in spite of a deficit of the supporting electrolyte, and the results obtained show under which conditions it is possible.

If migration effects are present, they change the steady-state limiting currents by up to few tens percent (depending on the type of equilibrium and the charge numbers of the species), for relative ligand concentration changes from 0.1 to 10^4. The exceptions are the charge reversal processes, that can exhibit changes in the I_{lim} values by few hundred percent, but such processes are not often encountered in practice.

The complex compounds reacting with and without liberation of the ligand have practically identical characteristics if the changes in the conductivities, caused by the electrode reaction, are identical, and all the products have the same diffusion coefficients.

The variation of the halfwave potential, in the case of the outer-sphere complex reaction or the reaction of the uncomplexed form, with the concentration of the ligand is in order of few mV. There are only a few situations where such variations can be measurable. The departures from the symmetry of the wave are small and can not be used for the quantitative analysis.

For a number of situations, where migration plays a significant role in the transport, the fitted functions relating the normalized stability constant $\tilde{\beta}_{\mathrm{n}}$ to the normalized limiting current I_{lim}, reported in the paper, can be used. The analysis of various cases presented in the paper can be used for diagnostic purposes with respect to the experimental data. Validation of these theoretical results will be the subject of a future paper.

Therefore, it can be concluded that the electrochemical investigation of complexing equilibria for the inert complexes without addition of an uncharged electrolyte is feasible and the appropriate expressions linking the limiting current and the complex stability constant are available.

Acknowledgements

This work was supported in part by grants (BST-472/5/94 and BST-502/5/95) from the University of Warsaw. The allocation of computer resources of the Interdisciplinary Center of Mathematical and Computational Modelling (ICM), University of Warsaw, is gratefully acknowledged.

References

[1] L. Mignano, M. Perdicakis and J. Bessiere, Anal. Chim. Acta, 305 (1995) 137.
[2] S.R. Almquist, L. Nyholm and K.E. Markides, poster on 5th European Conference on ElectroAnalytical Chemistry, Venice, May 22-26, 1994.
[3] L. Nyholm and G. Wikmark, Anal. Chim. Acta, 273 (1993) 41.
[4] S. Daniele, M.A. Baldo, M. Corbetta and G.A. Mazzocchin, J. Electroanal. Chem., 379 (1994) 261.
[5] M. Ciszkowska, Z. Stojek, S.E. Morris and J.G. Osteryoung, Anal. Chem., 64 (1992) 2372.
[6] Z. Stojek, M. Ciszkowska and J.G. Osteryoung, Anal. Chem., 66 (1994) 1507.
[7] M. Ciszkowska and Z. Stojek, Analyst, 119 (1994) 239.
[8] M. Ciszkowska and Z. Stojek, J. Electroanal. Chem., 344 (1993) 135.
[9] C. Beriet and D. Pletcher, J. Electroanal. Chem., 361 (1993) 93.
[10] J.D. Norton, S.A. Anderson and H.S. White, J. Phys. Chem., 96 (1992) 3.

[11] C. Amatore, M.R. Deakin and R.M. Wightman, J. Electroanal. Chem., 255 (1987) 49.
[12] C. Amatore, J. Bartelt, M.R. Deakin and R.M. Wightman, J. Electroanal. Chem., 256 (1988) 255.
[13] K.B. Oldham, J. Electroanal. Chem., 250 (1988) 1.
[14] K.B. Oldham, J. Electroanal. Chem., 337 (1993) 91.
[15] D.R. Baker, M.W. Verbrugge and J. Newman, J. Electroanal. Chem., 314 (1991) 23.
[16] J.C. Myland and K.B. Oldham, J. Electroanal. Chem., 347 (1993) 49.
[17] J.D. Norton, H.S. White and S.W. Feldberg, J. Phys. Chem., 94 (1990) 6772.
[18] C.P. Smith and H.S. White, Anal. Chem., 65 (1993) 3343.
[19] S. Daniele, I. Lavagnini, M.A. Baldo and F. Magno, J. Electroanal. Chem., 404 (1996) 105.
[20] A. Jaworski, Z. Stojek and J. Osteryoung, Anal. Chem., 67 (1995) 34.
[21] M.V. Twigg (Ed.), Mechanisms of Inorganic and Organometallic Reactions, vol. 5, Plenum Press, New York, 1988, chapts. 5–8.
[22] J.D. Norton, W.E. Benson, H.S. White, B.D. Pendley and H.D. Abruna, Anal. Chem., 63 (1991) 1909.
[23] M. Palys, Z. Stojek, M. Bos and W.E. van der Linden, J. Electroanal. Chem., 383 (1995) 105.
[24] M. Bos and H.Q.J. Meershoek, Anal. Chim. Acta, 61 (1972) 185.
[25] S.W. Feldberg, J. Electroanal. Chem., 127 (1981) 1.
[26] W.H. Press, S.A. Teukolsky, W.T. Vetterling and B.P. Flannery, Numerical Recipes in C (2nd edition), Cambridge University Press, Cambridge, 1992, p. 683 .